ACCSCIENCE PUBLISHING

Eurasian Journal of Medicine and Oncology

ORIGINAL RESEARCH ARTICLE

# Exploratory analysis of CT-derived radiomic features and adipose tissue distribution in relation to lipid metabolism pathway activity in ovarian serous cystadenocarcinoma

**Federico Greco[1]*, Luca Giordano[2], Chiara Noemi Greco[2], Chiara Pallara[3], Luca Leo[2], Roberta Montefrancesco[2], and Arnaldo Scardapane[1]**

[1]Department of Experimental Medicine, College ISUFI, University of Salento, Monteroni, Lecce, Italy

[2]Department of Radiology, "Vito Fazzi" Hospital, Lecce, Italy

[3]Interdisciplinary Department of Medicine, Section of Radiology and Radiation Oncology, University of Bari "Aldo Moro", Bari, Italy

## Abstract

**Introduction**: Ovarian cancer is characterized by high recurrence rates and complex metabolic reprogramming. Lipid metabolism pathways may influence tumor imaging phenotypes and contribute to biologic heterogeneity.

**Objective**: This study investigated whether computed tomography (CT)-derived radiomic features are associated with metabolic activity profiles in ovarian cancer.

**Methods**: This retrospective radiogenomic study included 68 patients from the Cancer Genome Atlas Ovarian Cancer cohort with available contrast-enhanced CT imaging and matched transcriptomic data. Patients were stratified into high and low metabolic activity groups according to lipid metabolism-related pathway expression profiles. A two-dimensional radiomic approach was adopted using the axial CT slice showing the largest tumor area. Tumor regions were manually segmented, and handcrafted radiomic features were extracted using a custom pipeline developed in Python. Statistical comparisons between groups were performed using the Mann–Whitney U test with Benjamini–Hochberg false discovery rate (FDR) correction.

**Results**: Several radiomic features showed nominal or borderline differences between high- and low-metabolic-activity groups, including glcm_ASM_std ($p$ = 0.027), shape_perimeter_mm ($p$ = 0.045), glrlm_rln ($p$ = 0.049), shape_minor_axis_length_px ($p$ = 0.050), and intensity_p10_HU ($p$ = 0.053). Tumors with higher metabolic activity tended to exhibit larger morphologic dimensions and subtle texture alterations. Subcutaneous adipose tissue (SAT) demonstrated the strongest inverse correlation with LipidScore (Spearman rho = −0.24), and a non-significant trend toward higher SAT values was observed in the low-lipid-metabolism group ($p$ = 0.072). However, none of the radiomic features remained statistically significant after FDR correction.

**Conclusion**: CT-derived radiomic features showed weak exploratory associations with metabolic activity-related molecular profiles in ovarian cancer. Although no robust associations were confirmed after multiple-comparison correction, the observed trends suggest potential radiogenomic interactions related to tumor metabolism that warrant further investigation in larger cohorts.

***Corresponding author:**
Federico Greco
(federico.greco@unisalento.it)

**Citation:** Greco F, Giordano L, Greco CN, *et al*. Exploratory analysis of CT-derived radiomic features and adipose tissue distribution in relation to lipid metabolism pathway activity in ovarian serous cystadenocarcinoma. *Eurasian J Med Oncol*.
doi: 10.36922/EJMO026230260

**Received:** June 6, 2026

**Revised:** June 24, 2026

**Accepted:** July 17, 2026

**Published online:** November 16, 2026

**Copyright:** © 2026 Author(s). This is an Open-Access article distributed under the terms of the Creative Commons Attribution License, permitting distribution, and reproduction in any medium, provided the original work is properly cited.

**Publisher's Note:** AccScience Publishing remains neutral with regard to jurisdictional claims in published maps and institutional affiliations.

***Keywords:*** Adipose tissue; Lipid metabolism; Ovarian serous cystadenocarcinoma; Radiogenomics; Radiomics

## 1. Introduction

Growing evidence suggests that ovarian cancer (OC) cells undergo profound lipid metabolic reprogramming to sustain their increased energetic and biosynthetic demands. Alterations involving fatty acid uptake, transport, and utilization have been identified even in early phases of disease development and appear to become progressively more pronounced during tumor progression and metastatic dissemination.[1] Cellular lipid metabolism comprises a highly coordinated network of anabolic and catabolic processes that regulate the synthesis, uptake, transport, storage, and utilization of lipids in eukaryotic cells. These mechanisms are essential for maintaining metabolic equilibrium and supporting normal cell function. Increasing evidence indicates that alterations in lipid metabolic regulation contribute to the development and progression of several human disorders, including cancer, where metabolic reprogramming represents a hallmark of malignant transformation.[2] In OC, lipids participate in multiple biological processes, supporting the metabolic demands of rapidly proliferating tumor cells while influencing immune mechanisms within the tumor microenvironment.[2]

Metabolic reprogramming in OC is characterized by increased expression of enzymes involved in lipid biosynthesis, a process associated with tumor progression, metastatic dissemination, and maintenance of cancer cell viability. In particular, fatty acid synthase and stearoyl-CoA desaturase 1, which participate in fatty acid synthesis and desaturation, are commonly overexpressed in aggressive ovarian tumors, thereby promoting the accumulation of unsaturated fatty acids.[1,3,4] Increased lipid metabolic activity has been associated with a more aggressive tumor phenotype and unfavorable clinical outcomes. Therefore, a better understanding of lipid metabolic alterations may improve our knowledge of the molecular events driving OC progression and facilitate the identification of novel metabolism-based therapeutic strategies.[2] Besides *de novo* lipid synthesis, cancer cells also rely on the mobilization and utilization of intracellular lipid stores to support the metabolic processes required for tumor growth and progression. Several studies have reported increased expression of enzymes involved in lipid catabolism and fatty acid degradation in malignant cells compared with non-neoplastic tissues.[5-8] Interestingly, some of these enzymes participate in both lipid synthesis and lipid degradation. Acyl-CoA synthetase long chain family member 1 represents one such example, underscoring the complexity and metabolic plasticity of lipid regulation in cancer cells.[8]

Advances in quantitative image analysis have led to the development of radiomics, an approach that extracts numerous quantitative descriptors from routinely acquired medical images to characterize tumor phenotype and biological heterogeneity without the need for invasive procedures.[9,10] Radiomics has been increasingly applied across several aspects of ovarian tumor evaluation, including lesion characterization, histopathological assessment, prognostic stratification, and treatment response prediction, by capturing subtle imaging patterns and uncovering potentially hidden information not appreciable on conventional visual assessment.[11,12] Based on this background, we explored whether lipid metabolism pathway activity is associated with computed tomography (CT)-derived radiomic characteristics and abdominal adipose tissue distribution in ovarian serous cystadenocarcinoma. To address this question, an integrated radiogenomic analysis was performed using matched imaging and transcriptomic data from The Cancer Genome Atlas (TCGA) ovarian serous cystadenocarcinoma (TCGA-OV) and The Cancer Imaging Archive (TCIA).[13] Specifically, we sought to explore whether imaging-derived tumor phenotypes and body composition biomarkers may reflect lipid metabolic reprogramming in OC.

## 2. Materials and methods

### 2.1. Study design and patient selection

This retrospective radiogenomic investigation was based on publicly available matched imaging and transcriptomic datasets retrieved from the TCIA TCGA-OV collection and TCGA-OV project. Patients with ovarian serous cystadenocarcinoma from the TCGA-OV cohort were evaluated.[13] Although the TCGA-OV dataset is historically designated as ovarian serous cystadenocarcinoma, the vast majority of tumors included in this cohort correspond to high-grade serous ovarian carcinoma according to contemporary histopathologic classification.

Patients were selected on the basis of predefined eligibility criteria, including availability of preoperative CT imaging and availability of matched gene-expression data. Patients without preoperative CT imaging or without available genomic data were excluded. Additional exclusion

criteria included lesions that were entirely cystic without a visible solid component suitable for segmentation, severely artifacted or incomplete CT examinations, and examinations lacking the anatomical slices required for adipose tissue quantification, specifically the slice located approximately 3 cm above the inferior endplate of the third lumbar vertebra (L3).

Initially, 93 patients with available CT imaging were identified. After radiogenomic matching and exclusion of cases without complete transcriptomic profiling, the final study population consisted of 68 patients with matched imaging and genomic data.

The study exclusively used anonymized data available in publicly accessible repositories. Therefore, neither institutional ethics committee approval nor informed consent was required, in accordance with TCGA and TCIA policies and the principles outlined in the Declaration of Helsinki. No specific ethics approval number was required or available for this study.

### 2.2. Computed tomography imaging analysis and abdominal adipose tissue quantification

Computed tomography examinations were retrieved from TCIA and reviewed using Horos software (version 4.0.0 RC2, Horos Project, USA). CT examinations were obtained from multiple institutions through TCIA. Owing to the retrospective multicenter nature of the dataset, acquisition parameters such as scanner manufacturer, reconstruction kernel, slice thickness, and imaging protocols were not fully standardized across all cases. All analyses were performed on contrast-enhanced CT examinations acquired during the venous phase. Quantification of abdominal adipose tissue compartments, including total adipose tissue (TAT), visceral adipose tissue (VAT), and subcutaneous adipose tissue (SAT), was performed using a semi-automated segmentation tool implemented in Horos software. The software identified adipose tissue based on standard fat attenuation values in Hounsfield units (HU). Segmentation results were visually reviewed and manually adjusted when necessary to ensure accurate delineation of adipose tissue compartments. Adipose tissue measurements were reported as absolute cross-sectional areas ($cm^2$) and were not normalized for height, body surface area, or other anthropometric parameters. Adipose tissue distribution was quantified on a single axial CT image obtained approximately 3 cm cranial to the inferior border of L3, using a previously described single-slice body composition quantification method.[14] Adipose tissue areas were measured in square centimeters ($cm^2$). In addition, VAT/SAT ratios were calculated as surrogate indicators of adipose tissue distribution.

### 2.3. Tumor segmentation

For radiomic analysis, the solid tumor component was manually segmented on a single representative axial CT slice demonstrating the largest visible tumor area. Tumor segmentation was carried out by a board-certified radiologist experienced in abdominal and oncologic imaging using the pencil tool available in Horos software. No independent second-reader segmentation was performed, and inter-reader agreement was therefore not assessed. The aim of segmentation was to encompass the entire visible tumor lesion. Consequently, intratumoral cystic or necrotic areas contained within the lesion boundaries were included in the region of interest (ROI), whereas external non-contiguous components were excluded. This approach was adopted to provide a comprehensive representation of tumor morphology and texture while maintaining methodological consistency across the study cohort. Cases without an identifiable solid component were excluded from the analysis. ROIs were manually delineated and exported in .roi format for subsequent radiomic processing. A two-dimensional segmentation approach based on the largest axial tumor section was selected to ensure methodological consistency across all cases and to facilitate reproducible manual segmentation in this exploratory radiogenomic study.

### 2.4. Radiomic feature extraction

Radiomic feature extraction, data processing, statistical analyses, and multiple-comparison correction were performed using a custom pipeline developed in Python (3.13.5, Python Software Foundation, Netherlands). Prior to feature extraction, all ROIs and corresponding CT images were visually reviewed to ensure correct image–segmentation matching and segmentation quality.

Radiomic features were extracted from the segmented tumor regions using standardized extraction settings across the entire cohort. A total of 40 radiomic features were extracted, including shape-based features, first-order intensity statistics, gray-level co-occurrence matrix (GLCM) features, gray-level run-length matrix (GLRLM) features, gray-level size-zone matrix features, gray-level dependence matrix features, and neighboring gray-tone difference matrix features. The study was designed as an exploratory feature-level analysis; therefore, no feature-selection or dimensionality-reduction strategy was applied before statistical testing.

The extracted radiomic features belonged to commonly used radiomic feature classes, including first-order, shape, GLCM, GLRLM, gray-level size-zone matrix, gray-level dependence matrix, and neighboring gray-tone difference matrix features, which are also described within the Image

Biomarker Standardisation Initiative framework. However, formal verification of Image Biomarker Standardisation Initiative compliance was not performed.

No image resampling, intensity normalization, or feature standardization procedures were applied prior to feature extraction. Radiomic features were extracted using identical processing settings across all cases.

### 2.5. Lipid metabolism pathway analysis

Transcriptomic data from the TCGA-OV cohort were obtained through the TCGA/cBioPortal framework. Gene-expression data were obtained using the normalized transcriptomic values provided by the database. No additional normalization procedures or batch-effect correction were performed by the investigators. Lipid metabolism pathway activity was assessed using the Molecular Signatures Database (MSigDB) Hallmark gene set (HALLMARK_FATTY_ACID_METABOLISM), which includes genes involved in fatty acid transport, β-oxidation, lipid synthesis, and cellular fatty acid metabolism. The original Hallmark pathway comprised 156 genes. During transcriptomic data retrieval and preprocessing, genes located on sex chromosomes were automatically excluded by the platform, including *ACSL4*, *HCCS*, *HSD17B10*, *IDH3G*, *MAOA*, *NSDHL*, *PDHA1*, and *SMS*. Consequently, the final pathway analysis was performed using 148 genes. The exclusion of these genes was not performed manually by the investigators but resulted from the transcriptomic preprocessing pipeline used for data retrieval. Although these genes are involved in lipid metabolism, their exclusion affected only a small proportion of the original Hallmark pathway and was unlikely to substantially alter the overall biological interpretation of pathway activity.

For each patient, a lipid metabolism pathway score (LipidScore) was calculated as the mean expression value of the pathway-related genes. This approach was selected to provide a simple and transparent summary measure of pathway activity suitable for exploratory radiogenomic analysis. Alternative pathway-scoring approaches, including Gene Set Variation Analysis and single-sample Gene Set Enrichment Analysis, were not applied and may represent valuable directions for future investigations. The study cohort was then divided into high- and low-lipid-metabolism groups using the median LipidScore as the classification threshold.

### 2.6. Statistical analysis

According to data distribution, continuous variables were summarized using either mean ± standard deviation or median and interquartile range. Associations between adipose tissue measurements, radiomic features, and LipidScore were evaluated using Spearman correlation analysis. Differences between the high- and low-lipid-metabolism groups were evaluated using the Mann–Whitney *U* test.

To account for multiple comparisons, Benjamini–Hochberg false discovery rate (FDR) correction was applied to the 40 radiomic comparisons performed between the high- and low-lipid-metabolism groups. Adjusted FDR *q*-values were calculated and reported alongside nominal *p*-values. Rank-biserial correlation coefficients, together with their corresponding 95% confidence intervals, were calculated to quantify effect size. Statistical significance was defined as a two-tailed *p*-value below 0.05. To assess the potential confounding effects of clinical variables, multivariable linear regression analyses were performed for the radiomic features showing the strongest nominal associations with the lipid metabolism group. Each radiomic feature was entered as the dependent variable, while lipid metabolism group, age, stage, and residual disease status were included as independent variables.

## 3. Results

### 3.1. Study population

The TCGA-OV dataset initially included 93 patients with preoperative CT scans available through TCIA, all of whom were considered for radiogenomic matching. After radiogenomic matching with transcriptomic data and exclusion of patients lacking complete genomic information, the final radiogenomic cohort consisted of 68 patients with both evaluable CT imaging and matched gene-expression data. Table 1 summarizes the clinical characteristics of the study cohort. The mean age of the cohort was 59.2 ± 10.7 years (range, 40–80 years). Most patients presented with advanced-stage disease, with Stage IIIC representing the most frequent category.

### 3.2. Lipid metabolism pathway analysis

Lipid metabolism pathway activity was evaluated using the MSigDB Hallmark gene set (HALLMARK_FATTY_ACID_METABOLISM). After excluding sex chromosome-related genes automatically removed during preprocessing, the final analysis included 148 pathway-related genes.

For each patient, a LipidScore was calculated as the mean expression value of the pathway-associated genes. Using the median LipidScore as the cutoff, patients were classified into high- and low-lipid-metabolism groups, yielding two equally sized cohorts of 34 patients each.

Individuals in the high-lipid-metabolism group were significantly younger than those classified in the low-

**Table 1. Clinical characteristics of the study population according to lipid metabolism status**

| Variable | Category | High lipid metabolism ($n$ = 34) | Low lipid metabolism ($n$ = 34) | $p$-value |
|---|---|---|---|---|
| Age (years) | Mean ± SD | 62.8 ± 9.4 | 55.9 ± 10.9 | 0.024 |
| Clinical stage | Early (I–II) | 3 (8.8%) | 2 (5.9%) | 1.000 |
| | Advanced (III–IV) | 31 (91.2%) | 32 (94.1%) | |
| Residual disease | <1 cm | 17 (50.0%) | 14 (41.2%) | 0.745 |
| | >1 cm | 6 (17.6%) | 7 (20.6%) | |
| | Not available | 11 (32.4%) | 13 (38.2%) | |

Notes: Continuous variables are reported as mean ± standard deviation (SD), while categorical variables are presented as counts (percentages); comparisons between groups were performed using the Mann–Whitney $U$ test for continuous variables and Fisher's exact test for categorical variables. A statistically significant difference in age was observed between groups, whereas no significant differences were identified for clinical stage or residual disease.

lipid-metabolism group (57.6 ± 11.0 vs. 63.5 ± 10.5 years, $p$ = 0.024). No statistically significant differences were observed regarding advanced clinical stage (91.2% vs. 94.1%, $p$ = 1.000) or residual disease > 1 cm (17.6% vs. 20.6%, $p$ = 0.745).

### 3.3. Abdominal adipose tissue analysis

Correlation analyses demonstrated exploratory associations between abdominal adipose tissue compartments and LipidScore. SAT showed the strongest inverse correlation with LipidScore (Spearman rho = −0.24), followed by TAT (rho = −0.21) and VAT (rho = −0.16). Although these associations did not reach statistical significance, the observed trends suggested that higher adipose tissue values tended to be associated with lower lipid metabolism pathway activity. Comparisons between high- and low-lipid-metabolism groups demonstrated higher SAT values in the low-lipid-metabolism group, with a near-significant difference ($p$ = 0.072; Figure 1).

### 3.4. Radiomic analysis

Radiomic feature extraction was successfully performed in all 68 patients included in the final radiogenomic cohort. A total of 40 radiomic features were evaluated, resulting in 40 statistical comparisons between the high- and low-lipid-metabolism groups. To reduce the risk of false-positive findings arising from multiple statistical tests, the Benjamini–Hochberg FDR approach was applied. Adjusted q-values obtained from this correction are shown in Table 2.

Among all evaluated features, glcm_ASM_std showed the lowest nominal $p$-value ($p$ = 0.0268), followed by shape_perimeter_mm ($p$ = 0.0449) and glrlm_rln ($p$ = 0.0490). However, none of the evaluated features remained statistically significant after Benjamini–Hochberg correction (lowest $q$-value = 0.3618).

To assess the potential confounding effects of age and clinical variables, additional multivariable linear regression analyses were performed for the radiomic features showing the strongest nominal associations. After adjustment for age, stage, and residual disease status, glcm_ASM_std remained nominally associated with lipid metabolism group ($p$ = 0.028), whereas shape_perimeter_mm ($p$ = 0.123), glrlm_rln ($p$ = 0.215), shape_minor_axis_length_px ($p$ = 0.104), and intensity_p10_HU ($p$ = 0.131) did not retain nominal statistical significance.

Several exploratory differences in radiomic features were observed between the high- and low-lipid-metabolism groups. Among texture-derived features, glcm_ASM_std demonstrated the strongest nominal association with metabolic activity, suggesting differences in local texture uniformity between the two groups. Additional nominal associations were observed for glrlm_rln, indicating potential alterations in gray-level run-length heterogeneity, and for the shape-related parameter shape_perimeter_mm, suggesting subtle differences in tumor morphology (Figure 2). Borderline associations were also identified for shape_minor_axis_length_px ($p$ = 0.0504) and the first-order attenuation feature intensity_p10_HU ($p$ = 0.0525).

Overall, these findings should be considered exploratory and hypothesis-generating. Although several radiomic features demonstrated nominal associations with lipid metabolism pathway activity, none remained statistically significant after FDR correction. Therefore, these observations may represent potential trends requiring validation in larger independent cohorts.

Exploratory Pearson correlation analysis was

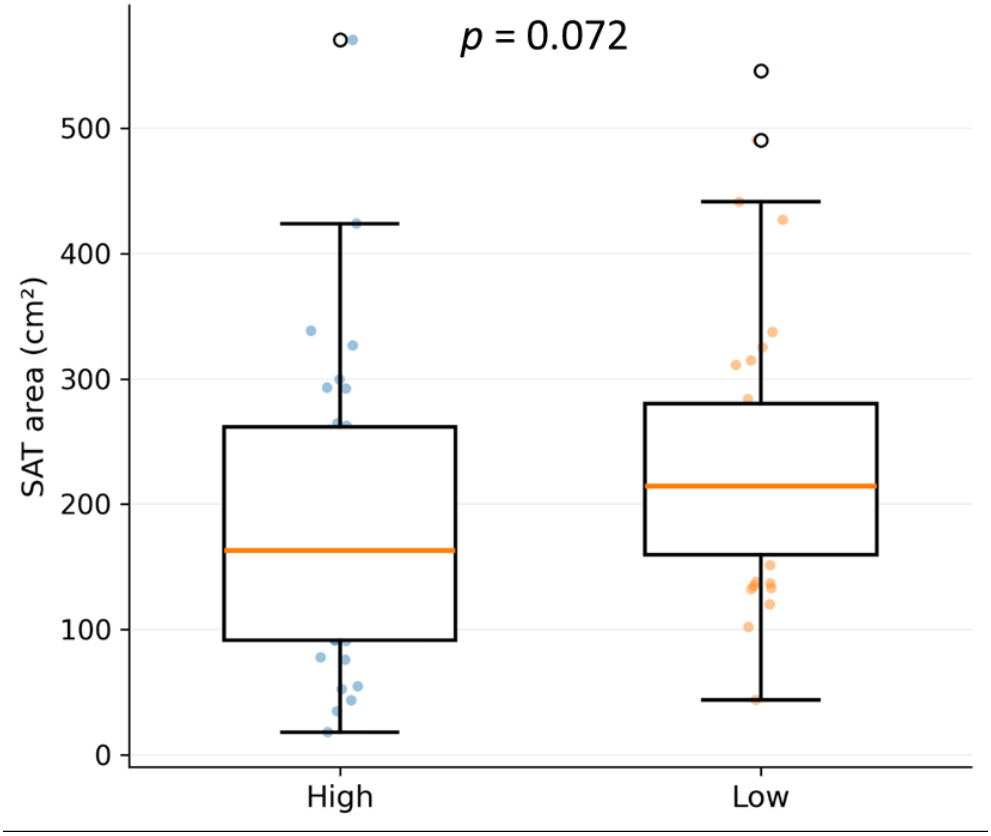



**Figure 1.** Boxplot showing the distribution of subcutaneous adipose tissue (SAT) area between high and low metabolic activity groups in ovarian cancer patients. The low metabolic activity group demonstrated a trend toward higher SAT values compared with the high metabolic activity group; however, the difference did not reach statistical significance (Mann–Whitney *U* test, $p = 0.072$). Individual patient values are overlaid on the boxplots.

**Table 2. Radiomic features showing the strongest nominal associations with lipid metabolism pathway activity in ovarian serous cystadenocarcinoma**

| Feature | High lipid metabolism (median) | Low lipid metabolism (median) | *p*-value | FDR *q*-value | Rank-biserial *r* (95% CI) |
|---|---|---|---|---|---|
| glcm_ASM_std | 0.0048 | 0.0062 | 0.0268 | 0.3618 | −0.313 (−0.566, −0.045) |
| shape_perimeter_mm | 195.06 | 149.99 | 0.0449 | 0.3618 | 0.284 (0.009, 0.543) |
| glrlm_rln | 4,406.51 | 2,944.64 | 0.0490 | 0.3618 | 0.279 (0.005, 0.535) |
| shape_minor_axis_length_px | 51.23 | 43.41 | 0.0504 | 0.3618 | 0.277 (0.003, 0.531) |
| intensity_p10_HU | 36.00 | 30.00 | 0.0525 | 0.3618 | 0.274 (0.001, 0.535) |

Notes: Values are reported as medians for the high- and low-lipid-metabolism groups; statistical comparisons were performed using the Mann–Whitney *U* test. Benjamini–Hochberg FDR correction was applied to all 40 radiomic comparisons, and adjusted q-values are reported. Effect sizes are presented as rank-biserial correlation coefficients with corresponding 95% CIs. None of the evaluated features remained statistically significant after FDR correction. Abbreviations: ASM: Angular second moment; CI: Confidence interval; FDR: False discovery rate; HU: Hounsfield unit.

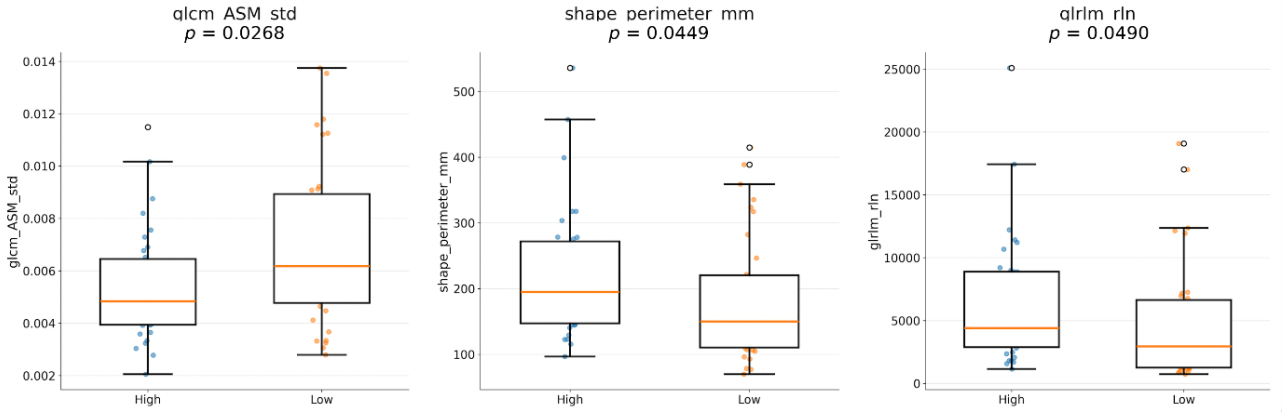



**Figure 2.** Boxplot comparison of the three radiomic features most strongly associated with lipid metabolism pathway activity between high- and low-metabolic-activity groups. The high metabolic activity group showed lower glcm_ASM_std values, suggesting reduced texture uniformity, along with higher shape_perimeter_mm and glrlm_rln values, potentially reflecting increased morphological complexity and altered intratumoral texture patterns. Statistical comparisons were performed using the Mann–Whitney *U* test. Although these features showed nominal statistical significance (glcm_ASM_std, $p = 0.0268$; shape_perimeter_mm, $p = 0.0449$; glrlm_rln, $p = 0.0490$), none remained significant after false discovery rate correction.
Abbreviation: ASM: Angular second moment.

subsequently performed to investigate potential associations between adipose tissue compartments and radiomic features showing nominal differences according to lipid metabolic activity. Among these features, shape_perimeter_mm demonstrated the strongest association with SAT, showing a trend toward an inverse correlation ($r = -0.234$, $p = 0.054$) (Figure 3). Given the weak magnitude of the correlation and the lack of statistical significance, this observation should be considered exploratory and hypothesis-generating. No significant correlations were identified for the remaining radiomic parameters.

## 4. Discussion

Exploratory radiogenomic analysis identified nominal, non-FDR-significant differences in selected CT-derived radiomic features according to lipid metabolism pathway activity in OC. Comparative analysis between high- and low-metabolic-activity groups identified differences in several radiomic features related to tumor texture and morphology, including glcm_ASM_std, glrlm_rln, and shape_perimeter_mm. In particular, lower glcm_ASM_std values observed in the high metabolic activity group may reflect reduced directional variability of texture uniformity within the tumor. Conversely, higher glrlm_rln values may indicate increased run-length heterogeneity and greater structural complexity within metabolically active tumors.

Interestingly, the shape-related radiomic feature shape_perimeter_mm demonstrated both nominal differences between metabolic groups and the strongest association with SAT. Since shape_perimeter_mm reflects contour complexity and morphological irregularity, this finding may suggest that lipid metabolic reprogramming influences not only tumor texture but also macroscopic architectural organization. Furthermore, exploratory Pearson correlation analysis demonstrated a trend toward an inverse association between SAT and shape_perimeter_mm ($r = -0.234$, $p = 0.054$), suggesting that tumors arising in patients with lower SAT values may exhibit greater morphological complexity and contour irregularity. Collectively, these findings may indicate potential relationships between systemic adiposity, lipid metabolic activity, and CT-derived tumor phenotypes; however, these observations should be interpreted cautiously given the lack of statistical significance after multiple-comparison correction.

Because age differed significantly between the two lipid metabolism groups, multivariable analyses were additionally performed to determine whether age and other clinical variables influenced the observed associations. After adjustment for age, stage, and residual disease status, only glcm_ASM_std retained a nominal association with lipid metabolism group, whereas the remaining radiomic features did not. These findings suggest that clinical factors may partially contribute to some of the observed radiomic differences and further support the exploratory nature of the present results.

Although several radiomic features demonstrated nominal associations with lipid metabolism pathway activity, none remained statistically significant after FDR correction. Consequently, the present findings should be regarded as exploratory and hypothesis-generating

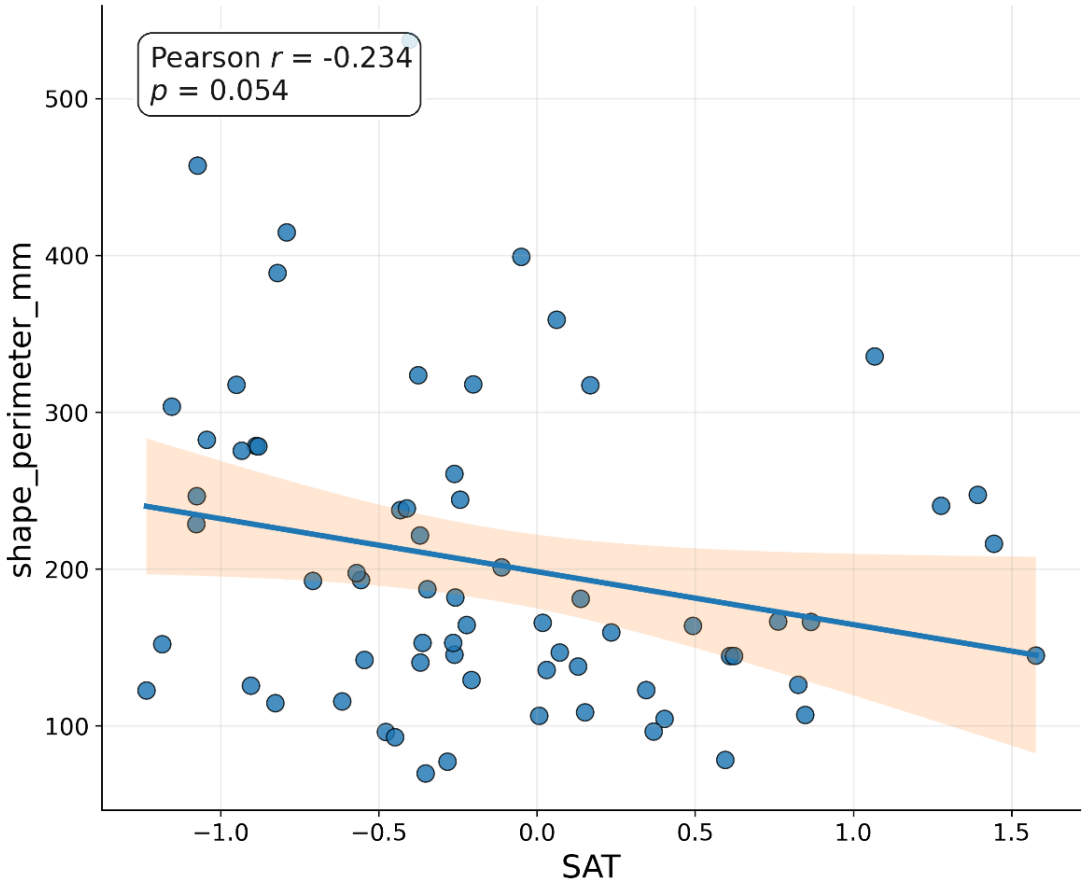



**Figure 3.** Scatter plot illustrating the exploratory correlation between subcutaneous adipose tissue (SAT) and the radiomic feature shape_perimeter_mm in The Cancer Genome Atlas ovarian serous cystadenocarcinoma cohort. shape_perimeter_mm is a shape-based radiomic parameter reflecting the overall complexity and extent of the tumor contour. A trend toward an inverse association was observed (Pearson $r = -0.234$, $p = 0.054$), suggesting that tumors arising in patients with lower SAT values may exhibit greater morphological complexity and contour irregularity. The solid line represents the linear regression fit, while the shaded area indicates the 95% confidence interval.

rather than evidence of robust radiogenomic interactions. These observations may provide a rationale for future studies investigating whether metabolic pathway activity contributes to identifiable CT-derived phenotypic signatures. Further validation in larger cohorts is needed to determine whether radiomics can serve as a reliable non-invasive tool for exploring tumor metabolic behavior. An additional methodological consideration relates to the calculation of LipidScore. In the present study, pathway activity was estimated as the mean expression of genes included in the MSigDB Hallmark Fatty Acid Metabolism gene set. Although this approach provides a simple and interpretable summary metric, it does not account for potential differences in gene weighting, variance, or biological contribution within the pathway. More advanced enrichment-based methods, such as Gene Set Variation Analysis or single-sample Gene Set Enrichment Analysis, may provide a more refined estimation of pathway activity and should be explored in future studies. In addition, dichotomizing LipidScore at the median may reduce statistical power and obscure potentially relevant continuous biological gradients.

Radiogenomics is a field of medical imaging that aims to identify associations between imaging phenotypes and the underlying genomic characteristics of diseases. Imaging phenotypes may be regarded as macroscopic manifestations of molecular processes that are detectable through medical imaging techniques.[15] The development of radiogenomics has closely paralleled the evolution of

precision medicine and can be viewed as the convergence of advanced medical imaging and genomic sciences.[16] By integrating medical imaging with genomic data, radiogenomics aims to uncover relationships between imaging phenotypes and the molecular mechanisms that shape disease biology.[17] More recently, the scope of radiogenomics has expanded beyond the exclusive analysis of genomic data. Contemporary approaches increasingly incorporate radiomic features with proteomic, metabolomic, and other biological datasets, reflecting a broader multi-omics framework aimed at capturing the complex biological landscape of cancer.[18]

While previous OC radiogenomic studies have largely focused on prognostic biomarkers, treatment response, and individual genomic alterations[19], the present study explored radiogenomic associations at the level of a biologically relevant metabolic pathway. Furthermore, by integrating CT-derived radiomic features with adipose tissue distribution metrics and lipid metabolism pathway activity derived from transcriptomic data, this study expands current OC radiogenomic research toward the characterization of lipid metabolic phenotypes and their imaging correlates.

Alterations in fatty acid metabolism contribute to multiple stages of cancer development, including tumor initiation, sustained cell proliferation, and disease progression.[20-22] Lipid molecules are particularly important in malignant cells because they provide an energy source capable of sustaining the high metabolic demands of tumor growth while also helping cancer cells tolerate stress during metastatic spread.[23,24] Increasing evidence has emphasized the intricate relationship between adipose tissue and OC biology.[25] In addition to storing lipids, adipose tissue acts as a dynamic endocrine and metabolic organ that secretes adipokines and a variety of inflammatory signaling molecules.[26,27] These signaling molecules may promote chronic low-grade inflammation and modulate tumor metabolic pathways[28], thereby contributing to a microenvironment favorable to tumor development. Elevated circulating free fatty acid levels have also been associated with enhanced cell proliferation.[29] Lipidomic studies have identified characteristic alterations in the circulating lipid composition of patients with OC compared with healthy controls, including changes in the abundance of specific fatty acids, phospholipids, and triglycerides.[30] These metabolic changes are thought to facilitate membrane formation and intracellular signaling in malignant cells and may provide useful biomarkers for the diagnosis and monitoring of OC.[31]

According to Zhong *et al.*[32], OC is characterized by widespread alterations in fatty acid metabolism affecting SAT, plasma, and tumor tissue. Their results suggest that the tumor can reshape systemic lipid metabolism by modifying adipocyte biology, potentially creating a metabolic environment that favors cancer progression. Consistent with this hypothesis, significant changes in the fatty acid profile of SAT were identified in patients with OC.

The present findings may also be considered within the broader landscape of non-invasive biomarkers in OC research. Beyond imaging-derived phenotypes and transcriptomic pathway analyses, several systemic biomarkers have been investigated as potential tools for risk assessment and disease characterization. For example, Matuszczak *et al.*[33] recently reported that elevated blood molybdenum levels were associated with an increased risk of OC among *BRCA1* mutation carriers. Although this finding is not directly related to CT radiomics, lipid metabolism, or radiogenomic tumor characterization, it highlights the growing interest in non-invasive systemic biomarkers as complementary sources of biological information in OC research. In this context, blood-based biochemical markers may contribute to a more comprehensive biomarker framework alongside genetic, molecular, and imaging-derived parameters.[33]

Several enzymes implicated in OC progression are involved not only in lipid synthesis, but also in lipid degradation and fatty acid oxidation pathways, supporting the metabolic flexibility and energetic demands of tumor cells. Previous studies have demonstrated that highly metastatic OC cells exhibit altered lipidomic profiles and increased phospholipid production, while acyl-CoA synthetase long chain family member 1 overexpression has been associated with enhanced metastatic dissemination and tumor progression.[2,7] In addition, enzymes involved in inflammatory lipid metabolism, including arachidonate 5-lipoxygenase and cyclooxygenase-2, have been linked to tumor cell migration, angiogenesis, extracellular matrix remodeling, and poor clinical outcomes in OC.[1,34-38] Fatty acid β-oxidation pathways also appear to contribute to OC progression. Carnitine palmitoyl transferases are key regulators of mitochondrial fatty acid oxidation.[39] In OC, experimental inhibition of carnitine palmitoyltransferase 1 has been shown to impair tumor proliferation and induce apoptosis.[40] Taken together, these observations emphasize the importance of lipid metabolic alterations in OC biology and provide a biological rationale for the identification of metabolism-related imaging phenotypes.

Several limitations should nevertheless be acknowledged. First, the retrospective design, the relatively limited sample size ($n$ = 68), and the number of radiomic features evaluated ($n$ = 40) may have reduced

statistical power, particularly after multiple-comparison correction. Consequently, modest associations may have remained undetected, and false-positive findings cannot be completely excluded. Therefore, larger studies will be necessary to improve statistical power and validate the observed findings. Second, the use of a single-slice two-dimensional radiomic approach may not fully capture the entire spatial heterogeneity of ovarian tumors. OCs frequently contain solid, cystic, necrotic, hemorrhagic, and stromal components that may not be fully represented on a single axial section. Furthermore, imaging data were obtained from a multicenter public database, resulting in variability in CT acquisition parameters that could not be completely controlled. Although identical image-processing procedures were applied across all cases, differences in acquisition protocols may have influenced the extracted radiomic features. Third, tumor segmentation was performed by a single experienced radiologist, and neither inter-reader nor intra-reader reproducibility was assessed. Consequently, the potential influence of segmentation variability on radiomic feature extraction could not be evaluated. This limitation may be particularly relevant for shape-based radiomic features, which are potentially more sensitive to contouring variability. Additionally, the study lacked an independent validation cohort, limiting the generalizability of the findings. Future studies involving larger independent cohorts and external validation datasets are warranted to confirm the reproducibility of the observed findings. Furthermore, intratumoral cystic and necrotic components were included within the segmented ROIs. Although this approach allowed assessment of the entire visible lesion, these components may have influenced intensity- and texture-based radiomic features and potentially diluted biologically relevant signals arising from viable tumor tissue. Future studies should evaluate how compartment-specific segmentation strategies affect radiogenomic associations. Moreover, although several nominal associations were observed, none of the radiomic features remained statistically significant after FDR correction, and therefore the results should be interpreted as hypothesis-generating. Importantly, the observed effect sizes and correlations were generally modest, limiting the biological and pathophysiological interpretability of the findings. Therefore, the present study cannot establish a definitive association between CT-derived radiomic features and lipid metabolism pathway activity in OC. Instead, the identified trends should be regarded as preliminary, hypothesis-generating observations that require validation in larger independent cohorts and through more comprehensive multi-omics approaches. In addition, we summarized lipid metabolism activity using a mean-expression pathway score and dichotomized it at the median. This strategy may have reduced statistical power and obscured potentially relevant continuous biological gradients. Finally, we inferred transcriptomic pathway activity from bulk RNA sequencing data, which may not fully reflect the complex metabolic interactions occurring within the tumor microenvironment. Future studies involving larger independent cohorts and external validation datasets are warranted to confirm the reproducibility of the observed findings.

## 5. Conclusion

This exploratory radiogenomic study identified nominal, non-FDR-significant differences in selected CT-derived radiomic features according to lipid metabolism pathway activity in ovarian serous cystadenocarcinoma. Trends involving texture- and shape-related radiomic features, including glcm_ASM_std, glrlm_rln, and shape_perimeter_mm, were observed. A trend toward an inverse association between SAT and tumor contour complexity was also identified. Although none of these findings remained statistically significant after multiple-comparison correction, they should be considered hypothesis-generating observations warranting further investigation in larger independent cohorts. Further studies are needed to determine whether lipid metabolic activity is associated with reproducible CT-derived imaging phenotypes in OC.

## Acknowledgments

The authors acknowledge The Cancer Genome Atlas (TCGA) Research Network and The Cancer Imaging Archive (TCIA) for providing access to the clinical, genomic, and imaging data used in this study. The results shown here are in whole or in part based upon data generated by the TCGA Research Network: http://cancergenome.nih.gov/. The authors also thank the developers of the Horos imaging software for providing a free and open-source platform for medical image analysis.

## Funding

None.

## Conflict of interest

The authors declare no conflicts of interest to report regarding the present study.

## Author contributions

*Conceptualization*: Federico Greco
*Data curation:* Federico Greco
*Formal analysis:* Federico Greco
*Investigation:* Federico Greco
*Methodology:* Federico Greco

*Project Administration:* Federico Greco
*Software:* Federico Greco, Chiara Noemi Greco, Chiara Pallara
*Supervision:* Federico Greco, Arnaldo Scardapane
*Validation:* Federico Greco, Arnaldo Scardapane
*Visualization:* Federico Greco, Luca Giordano, Luca Leo, Roberta Montefrancesco
*Writing–original draft preparation:* Federico Greco
*Writing–review & editing:* Federico Greco

## Ethics approval and consent to participate

This study used publicly accessible, de-identified data from The Cancer Genome Atlas (TCGA) and The Cancer Imaging Archive (TCIA). Therefore, no institutional ethics approval was required. All procedures were retrospective and conducted in accordance with the Declaration of Helsinki. Computed tomography images and patient data for ovarian serous cystadenocarcinoma were obtained from TCIA. The TCIA project had already received approval from the relevant Institutional Review Board. This subsequent retrospective analysis, based on anonymized and publicly available data, did not require additional review due to the protective measures previously implemented by TCIA.

## Consent for publication

The study was performed in accordance with the Declaration of Helsinki. The institutional ethical committee approved the study. All subjects enrolled provided a written informed consent to use their anonymized data for research purposes.

## Availability of data

The imaging and transcriptomic datasets analyzed during the current study are publicly available from The Cancer Imaging Archive (TCIA) and The Cancer Genome Atlas (TCGA). TCIA OC imaging data can be accessed at https://www.cancerimagingarchive.net/, while transcriptomic data are available through the TCGA/cBioPortal platform. All data used in this study are publicly accessible and were analyzed in accordance with the respective database policies.

## References

1. Ji Z, Shen Y, Feng X, *et al*. Deregulation of lipid metabolism: the critical factors in ovarian cancer. *Front Oncol*. 2020;10:593017.

   doi: 10.3389/fonc.2020.593017

2. Chaudhry S, Thomas SN, Simmons GE Jr. Targeting lipid metabolism in the treatment of ovarian cancer. *Oncotarget*. 2022;13(1):768-783.

   doi: 10.18632/oncotarget.28241

3. Jiang L, Fang X, Wang H, Li D, Wang X. Ovarian cancer-intrinsic fatty acid synthase prevents anti-tumor immunity by disrupting tumor-infiltrating dendritic cells. *Front Immunol*. 2018;9:2927.

   doi: 10.3389/fimmu.2018.02927

4. Li J, Condello S, Thomes-Pepin J, *et al*. Lipid desaturation is a metabolic marker and therapeutic target of ovarian cancer stem cells. *Cell Stem Cell*. 2017;20(3):303-314.e5.

   doi: 10.1016/j.stem.2016.11.004

5. Beloribi-Djefaflia S, Vasseur S, Guillaumond F. Lipid metabolic reprogramming in cancer cells. *Oncogenesis*. 2016;5(1):e189.

   doi: 10.1038/oncsis.2015.49

6. Zhao S, Cheng L, Shi Y, Li J, Yun Q, Yang H. MIEF2 reprograms lipid metabolism to drive progression of ovarian cancer through ROS/AKT/mTOR signaling pathway. *Cell Death Dis*. 2021;12(1):18.

   doi: 10.1038/s41419-020-03336-6

7. Zhang Q, Zhou W, Yu S, *et al*. Metabolic reprogramming of ovarian cancer involves ACSL1-mediated metastasis stimulation through upregulated protein myristoylation. *Oncogene*. 2021;40(1):97-111.

   doi: 10.1038/s41388-020-01516-4

8. Ma Y, Temkin SM, Hawkridge AM, *et al*. Fatty acid oxidation: an emerging facet of metabolic transformation in cancer. *Cancer Lett*. 2018;435:92-100.

   doi: 10.1016/j.canlet.2018.08.006

9. Meier A, Veeraraghavan H, Nougaret S, *et al*. Association between CT-texture-derived tumor heterogeneity, outcomes, and BRCA mutation status in patients with high-grade serous ovarian cancer. *Abdom Radiol (NY)*. 2019;44(6):2040-2047.

   doi: 10.1007/s00261-018-1840-5

10. Vargas HA, Veeraraghavan H, Micco M, *et al*. A novel representation of inter-site tumour heterogeneity from pre-treatment computed tomography textures classifies ovarian cancers by clinical outcome. *Eur Radiol*. 2017;27(9):3991-4001.

    doi: 10.1007/s00330-017-4779-y

11. Jian J, Li Y, Pickhardt PJ, *et al*. MR image-based radiomics to differentiate type I and type II epithelial ovarian cancers. *Eur Radiol*. 2021;31(1):403-410.

    doi: 10.1007/s00330-020-07091-2

12. Li H, Cai S, Deng L, *et al*. Prediction of platinum resistance for advanced high-grade serous ovarian carcinoma using MRI-based radiomics nomogram. *Eur Radiol*. 2023;33(8):5298-5308.

    doi: 10.1007/s00330-023-09552-w

13. Holback C, Jarosz R, Prior F, *et al*. The Cancer Genome Atlas Ovarian Cancer Collection (TCGA-OV). Published online 2016.

doi: 10.7937/K9/TCIA.2016.NDO1MDFQ

14. Noumura Y, Kamishima T, Sutherland K, Nishimura H. Visceral adipose tissue area measurement at a single level: can it represent visceral adipose tissue volume? *Br J Radiol*. 2017;90(1077):20170253.

doi: 10.1259/bjr.20170253

15. Greco F, Panunzio A, Bernetti C, Tafuri A, Beomonte Zobel B, Mallio CA. Exploring the ADAM12 expression in clear cell renal cell carcinoma: a radiogenomic analysis on CT imaging. *Acad Radiol*. 2024;31(9):3672-3677.

doi: 10.1016/j.acra.2024.02.032

16. Liu Z, Duan T, Zhang Y, *et al*. Radiogenomics: a key component of precision cancer medicine. *Br J Cancer*. 2023;129(5):741-753.

17. Song L, Zhu Z, Mao L, *et al*. Clinical, conventional CT and radiomic feature-based machine learning models for predicting ALK rearrangement status in lung adenocarcinoma patients. *Front Oncol*. 2020;10:369.

doi: 10.3389/fonc.2020.00369

18. Peeken JC, Bernhofer M, Wiestler B, *et al*. Radiomics in radiooncology—challenging the medical physicist. *Phys Med*. 2018;48:27-36.

doi: 10.1016/j.ejmp.2018.03.012

19. Zeng S, Wang XL, Yang H. Radiomics and radiogenomics: extracting more information from medical images for the diagnosis and prognostic prediction of ovarian cancer. *Mil Med Res*. 2024;11(1).

doi: 10.1186/s40779-024-00580-1

20. Hanahan D, Weinberg RA. Hallmarks of cancer: the next generation. *Cell*. 2011;144(5):646-674.

doi: 10.1016/j.cell.2011.02.013

21. Wishart DS. Metabolomics for investigating physiological and pathophysiological processes. *Physiol Rev*. 2019;99(4):1819-1875.

doi: 10.1152/physrev.00035.2018

22. Martínez-Reyes I, Chandel NS. Cancer metabolism: looking forward. *Nat Rev Cancer*. 2021;21(10):669-680.

doi: 10.1038/s41568-021-00378-6

23. Corn KC, Windham MA, Rafat M. Lipids in the tumor microenvironment: from cancer progression to treatment. *Prog Lipid Res*. 2020;80:101055.

doi: 10.1016/j.plipres.2020.101055

24. Calder PC. Functional roles of fatty acids and their effects on human health. *JPEN J Parenter Enteral Nutr*. 2015;39(1 suppl):18S-32S.

doi: 10.1177/0148607115595980

25. Avgerinos KI, Spyrou N, Mantzoros CS, Dalamaga M. Obesity and cancer risk: emerging biological mechanisms and perspectives. *Metabolism*. 2019;92:121-135.

doi: 10.1016/j.metabol.2018.11.001

26. Iyengar NM, Hudis CA, Dannenberg AJ. Obesity and cancer: local and systemic mechanisms. *Annu Rev Med*. 2015;66(1):297-309.

doi: 10.1146/annurev-med-050913-022228

27. Brown KA, Scherer PE. Update on adipose tissue and cancer. *Endocr Rev*. 2023;44(6):961-974.

doi: 10.1210/endrev/bnad015

28. Vona-Davis L, Rose DP. The obesity-inflammation-eicosanoid axis in breast cancer. *J Mammary Gland Biol Neoplasia*. 2013;18(3-4):291-307.

doi: 10.1007/s10911-013-9299-z

29. Kolb H. Obese visceral fat tissue inflammation: from protective to detrimental? *BMC Med*. 2022;20(1):494.

doi: 10.1186/s12916-022-02672-y

30. Sah S, Bifarin OO, Moore SG, *et al*. Serum lipidome profiling reveals a distinct signature of ovarian cancer in Korean women. *Cancer Epidemiol Biomarkers Prev*. 2024;33(5):681-693.

doi: 10.1158/1055-9965.EPI-23-1293

31. Li Y, Shang C, Liang H, Zhang K, Wu Y, Guo H. Associations of novel serum lipid index with epithelial ovarian cancer chemoresistance and prognosis. *Front Oncol*. 2023;13:1052760.

doi: 10.3389/fonc.2023.1052760

32. Zhong X, Bilal M, Zhou Y, *et al*. Elucidating the role of fatty acid reprogramming in ovarian cancer: insights cross-talk between blood, subcutaneous fat, and ovarian cancer tissues. *Front Oncol*. 2025;15:1530487.

doi: 10.3389/fonc.2025.1530487

33. Matuszczak M, Kiljańczyk A, Marciniak W, *et al*. Blood molybdenum level as a marker of cancer risk on BRCA1 carriers. *Hered Cancer Clin Pract*. 2024;22(1).

doi: 10.1186/s13053-024-00291-7

34. Wen Z, Liu H, Li M, *et al*. Increased metabolites of 5-lipoxygenase from hypoxic ovarian cancer cells promote tumor-associated macrophage infiltration. *Oncogene*. 2015;34(10):1241-1252.

doi: 10.1038/onc.2014.85

35. Rocconi RP, Kirby TO, Seitz RS, *et al*. Lipoxygenase pathway receptor expression in ovarian cancer. *Reprod Sci*. 2008;15(3):321-326.

doi: 10.1177/1933719108316390

36. Ghosh N, Chaki R, Mandal V, Mandal SC. COX-2 as a target for cancer chemotherapy. *Pharmacol Rep*. 2010;62(2):233-244.

doi: 10.1016/S1734-1140(10)70262-0

37. Gu P, Su Y, Guo S, *et al*. Over-expression of COX-2 induces human ovarian cancer cells (CAOV-3) viability, migration and proliferation in association with PI3-k/Akt activation. *Cancer Invest*. 2008;26(8):822-829.

doi: 10.1080/07357900801941860

38. Wang YP, Wang QY, Li CH, Li XW. COX-2 inhibition by celecoxib in epithelial ovarian cancer attenuates E-cadherin suppression through reduced Snail nuclear translocation. *Chem Biol Interact*. 2018;292:24-29.

doi: 10.1016/j.cbi.2018.06.020

39. Bonnefont JP, Djouadi F, Prip-Buus C, Gobin S, Munnich A, Bastin J. Carnitine palmitoyltransferases 1 and 2: biochemical, molecular and medical aspects. *Mol Aspects Med*. 2004;25(5-6):495-520.

doi: 10.1016/j.mam.2004.06.004

40. Shao H, Mohamed EM, Xu GG, *et al*. Carnitine palmitoyltransferase 1A functions to repress FoxO transcription factors to allow cell cycle progression in ovarian cancer. *Oncotarget*. 2016;7(4):3832-3846.

doi: 10.18632/oncotarget.6757